NeuroImage 205 (2020) 116304

Contents lists available at ScienceDirect

NeuroImage

journal homepage: www.elsevier.com/locate/neuroimage

Decomposing alpha and 1/f brain activities reveals their differential associations with cognitive processing speed

Guang Ouyang [a,*], Andrea Hildebrandt [b], Florian Schmitz [c,d], Christoph S. Herrmann [b]

[a] Faculty of Education, The University of Hong Kong, Hong Kong
[b] Department of Psychology, Carl von Ossietzky Universität Oldenburg, 26129, Oldenburg, Germany
[c] Institute of Psychology and Education, Ulm University, 89081, Ulm, Germany
[d] Department of Psychology, University of Duisburg-Essen, 45141, Essen, Germany

ARTICLE INFO

Keywords:
Alpha oscillation
1/f power law pattern
EEG
Cognitive processing speed

ABSTRACT

Research in cognitive neuroscience has extensively demonstrated that the temporal dynamics of brain activity are associated with cognitive functioning. The temporal dynamics mainly include oscillatory and 1/f noise-like, non-oscillatory brain activities that coexist in many forms of brain activity and confound each other's variability. As such, observed functional associations of narrowband oscillations might have been confounded with the broadband 1/f component. Here, we investigated the relationship between resting-state EEG activity and the efficiency of cognitive functioning in $N = 180$ individuals. We show that 1/f brain activity plays an essential role in accounting for between-person variability in cognitive speed – a relationship that can be mistaken as originating from brain oscillations using conventional power spectrum analysis. At first glance, the power of alpha oscillations appeared to be predictive of cognitive speed. However, when dissociating pure alpha oscillations from 1/f brain activity, only the 1/f predicted cognitive speed, whereas the predictive power of alpha vanished. With this highly powered study, we disambiguate the functional relevance of the 1/f power law pattern in resting state neural activities and substantiate the necessity of isolating the 1/f component from oscillatory activities when studying the functional relevance of spontaneous brain activities.

1. Introduction

Sustaining dynamic brain activities encode rich information about an individual's functional and cognitive profile (Valizadeh et al., 2019). One prominent feature of brain activity is that there are oscillations that occur at various levels of the neural system (Buzsaki, 2006). The functional relevance of brain oscillations has been widely studied both theoretically and experimentally (Arnal and Giraud, 2012; Wang, 2010). From a neurocognitive perspective, it is of great interest to explore how brain oscillations are related to cognitive performance outcomes. The most prominent oscillations measured from scalp EEG activity – the alpha oscillations – have been studied for a century, leading to a large body of findings on their functional roles and associations with cognitive performance outcomes (Babu Henry Samuel et al., 2018; Doesburg et al., 2016; Ergenoglu et al., 2004; Grandy et al., 2013; Haegens et al., 2011; Haegens et al., 2010; Hanslmayr et al., 2007; Ikkai et al., 2016; Kornrumpf et al., 2017; Lange et al., 2012; Linkenkaer-Hansen et al., 2004; Petro et al., 2019; Thut et al., 2006; Van Dijk et al., 2008; Weisz et al., 2014; Worden et al., 2000; Zhang and Ding, 2010). Available findings suggest that the relationship between alpha power and cognitive performance is multifaceted and not always linear: A negative within-person correlation has been observed in visual and somatosensory perception (Ergenoglu et al., 2004; Petro et al., 2019; Van Dijk et al., 2008; Weisz et al., 2014), a positive correlation has been observed for working memory (Haegens et al., 2010), and a U-shaped relationship has been found in somatosensory perception (Lange et al., 2012; Linkenkaer-Hansen et al., 2004; Zhang and Ding, 2010). Between-person relationships of alpha oscillations and cognitive performance have been extensively studied as well, leading to mixed findings (Bauml et al., 2008; Grandy et al., 2013; Hanslmayr et al., 2007; Klimesch, 1999; Klimesch et al., 2006; Mahjoory et al., 2019; Parameshwaran and Thiagarajan, 2017). The heterogeneity of alpha oscillations with respect to their generating sources (Basar, 2012; Klimesch, 1999; Palva and Palva, 2007) may partly account for the inconsistency that has been revealed in their functional relations. Another possible cause of the diverging results may lie in the mixture of alpha power with broadband background

* Corresponding author.
E-mail address: ouyangg@hku.hk (G. Ouyang).

https://doi.org/10.1016/j.neuroimage.2019.116304
Received 21 September 2019; Received in revised form 12 October 2019; Accepted 19 October 2019
Available online 22 October 2019

activity (Buzsaki, 2006; Wen and Liu, 2016b), which was not taken into consideration in many of the above mentioned studies.

In addition to oscillations, brain activity displays a dominant 1/f-like spectral pattern, reflecting a scale-free property (He, 2014; Van de Ville et al., 2010). Such an activity pattern has been ubiquitously observed in nature and has been linked to fundamental physical mechanisms (Bak et al., 1987). An important fact about the 1/f-like pattern of brain activity is that it is functionally relevant (Bassettt et al., 2006; Colombo et al., 2019; Dave et al., 2018; He, 2014; Palva et al., 2013; Podvalny et al., 2015; Tagliazucchi et al., 2013; Voytek et al., 2015; Waschke et al., 2017), which complicates the interpretation of the alpha-behavior relationships, because oscillatory (alpha) and non-oscillatory (1/f) activity components are mixed in recorded brain signals. Oscillatory and non-oscillatory activities are likely to be generated by distinct neural mechanisms and play different functional roles, which strongly calls for the necessity to disentangle them. Spectrum analysis (e.g., Fourier Transform) – a commonly used approach that measures the power of oscillations in a time series at different frequencies – disregards whether a true oscillatory pattern exists in the original time series or not (Bullock et al., 2003). Obviously, oscillatory power can be obtained from time series of pure noise as well. Another issue is that the estimated oscillatory power of brain signals contains a portion of 1/f noise,[1] even for the alpha band. Consequently, estimated within- or between-person relationships of oscillation power and cognitive performance outcomes can reflect either the oscillation part or the noise part of the brain signal. Attention to this issue has increased as reflected in an increasing amount of empirical and methodological studies that specifically emphasize this challenge (Demanuele et al., 2007; Haller et al., 2018; He et al., 2010a; McDonnell and Ward, 2011; Parameshwaran and Thiagarajan, 2017; Wen and Liu, 2016b). Therefore, it is imperative to disentangle oscillatory and non-oscillatory components of neural signals when studying their functional roles in cognition.

With the present study, we aimed to investigate the between-person relationship of power spectrum features (in resting-state EEG) and cognitive performance at a finer-grained level that would allow us to differentiate alpha oscillation from 1/f noise. Dissociating the two will undoubtedly help reveal a more detailed picture of functional signatures of ongoing brain activities. This is because the neural circuits or systems generating structured oscillations may rely on mechanistically different architectures in comparison with those that generate the 1/f noise (Buzsaki, 2006). To achieve our goal to separate oscillatory and non-oscillatory brain activity, we employed statistical approaches, combining structural equation modeling based on variance decomposition across persons with signal processing methods to disentangle alpha from 1/f noise. We report their differential associations with cognitive performance outcomes measured as cognitive processing speed. The reported novel findings help shed light on neural mechanisms underlying between-person differences in cognitive functioning efficiency.

2. Methods

2.1. Resting-state EEG recording

The resting EEG of the eyes-open and eyes-closed states (90 s each) were collected from 210 healthy young adults (18–40 years old, 105 women) seated in a sound-attenuated cabin. Informed consent was obtained from all participants, and this study received approval from the departmental ethics committee. EEG was recorded from 42 Ag/AgCl electrodes referenced to the left mastoid (A1). Forty electrodes were mounted on an elastic cap (Easycap, Brain Products, Germany) in accordance with the 10–20 system (Pivik et al., 1993). Two electrodes were positioned directly on the left (reference) and right mastoids. In addition, there was one right infra-orbital electrode and two electrodes positioned at the outer canthi of both eyes (EOG electrodes: VO2, HO1, HO2) intended to monitor blinks and eye movements. EEG data were amplified using BrainAmp DC amplifiers (Brain Products, Germany) with a 0.1 μV resolution, 5 kHz sampling rate, and 0.1–1000 Hz bandpass filter. They were recorded with the Brain Vision Recorder (Brain Products, Germany) while down-sampled to 1 KHz.

The pre-processing of continuous EEG data was conducted with the EEGLAB toolbox (version eeglab13_4_4b (Delorme and Makeig, 2004);). The data were down-sampled to 250 Hz. To remove artifacts due to blinks and eye movements, an independent component analysis (ICA; function: *runica*; algorithm: Infomax (Gradient)) was applied. SASICA (EEGLAB plugin (Chaumon et al., 2015);) was used as a guide for selecting the artifact components for rejection. The data were then low-pass filtered at 40 Hz and were re-referenced to average.

2.2. Object recognition task

Participants performed a simple object recognition task after the resting state EEG session. Despite the complexity of the experimental design (which consisted of multiple conditions), this task served to measure cognitive processing speed ability, which was captured by a latent factor in the psychometric analyses that were computed to extract cross-condition covariance (see below). Participants were asked to complete a familiarity decision task on objects they learned during a learning phase prior to the task session. The task consisted of 16 experimental conditions (each with 72 trials) in which the following dichotomous factors were manipulated: difficulty (two levels: easy and difficult), familiarity (two levels: familiar and unfamiliar), priming (two levels: primed and unprimed), and stimulus category (two levels: face and house). Performance was evaluated on the basis of the average RT in each condition of the task, resulting in 16 performance indicators that were used for latent variable modeling (see below).

Task difficulty was manipulated by varying the memory load. In the low memory load (easy) condition, only 12 stimuli had to be learned in the learning phase, whereas in the high memory load (difficult) condition, there were 36. In the learning phase, the target stimulus (unfamiliar to all participants) was presented for 5 s per stimulus in a randomized order for participants to memorize. Then, all familiarized stimuli were presented again in a randomized order, intermixed with new distractor stimuli, and participants had to indicate familiarity by pressing a button. This learning block was repeated with different orders of target stimuli and new unknown stimuli until the participant reached 100% accuracy in the low and 80% accuracy in the high memory load conditions, respectively. The task began thereafter. Familiarity was manipulated by presenting eight learned or unlearned images. Priming was manipulated by presenting a stimulus that was either the same (primed) or different (unprimed) from the target stimulus to be evaluated for its familiarity, before the presentation of the target stimulus (Fig. 1). Participants pressed the right key for familiar stimuli and the left key for unfamiliar stimuli. Object content was manipulated by introducing two categories of stimuli: faces and houses. Black and white portraits (50% women) were obtained from two external databases (Endl et al., 1998; Lundqvist et al., 1998) and our own database (Herzmann et al., 2010). All faces were shown from a frontal view with neutral expressions and gaze directed toward the viewer. They were fitted into a vertical ellipse of 200 × 300 pixels. House stimuli were also black and white and were fitted into a rectangular picture (landscape orientation) of 237 × 160 pixels. All face and house stimuli were matched in terms of overall luminance.

Each trial began with a black fixation cross presented for 1000 m s, followed by a prime stimulus for 500 m s. The prime was then replaced by a fixation circle displayed for 1300 m s, followed by the target stimulus for 2000 m s and an inter-trial interval of 200 m s. Participants were instructed to respond to the target stimulus as quickly and accurately as possible. An illustration of the paradigm is depicted in Fig. 1.

[1] In fact, the pattern should be described by $1/f^{\beta}$, where β is not necessarily equal to 1. For simplicity and convenience, here we used 1/f to refer to the general power-law pattern.

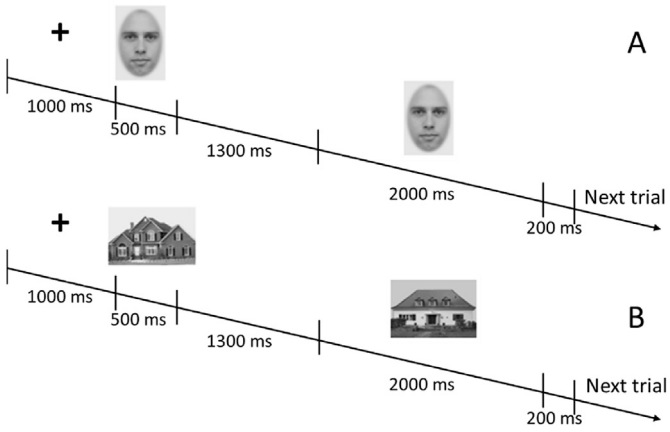

Fig. 1. The object recognition task. The first stimulus serves as priming information and is not task relevant. The second stimulus is the target stimulus and requires a decision by button press, indicating whether the stimulus is new or it has been learned at the beginning of a given task block. (A) Example of a primed trial in the face recognition tasks; (B) Example of an unprimed trial in the object (house) recognition tasks.

2.3. EEG spectrum analysis

The resting state EEG data were segmented into 90 epochs, each lasting for 1 s. We applied discrete Fast Fourier Transform (fft, Matlab R2016a) on each epoch and electrode to obtain the frequency spectrum. To exclude the non-stationary feature from the ongoing EEG activity, each 1-s epoch was detrended and demeaned. The discrete Fourier Transform was applied separately on each epoch with a transformation length that doubles the epoch length (by zero padding) to achieve a frequency resolution up to 0.5 Hz. Epochs containing amplitude variations of $> \pm 100\,\mu V$ were considered to contain abrupt jumping and were thus excluded from the analysis. The spectrum for each ten epochs were averaged to serve as one of the four indicators for structural equation modeling analysis (see below). In a first step, the scalp-averaged spectrum was used to study its relationship with behavioral performance. In a second step, the spatial specificity of the correlation between spectrum and behavior was examined.

2.4. Structural equation modeling

Three structural equation models (SEMs) were specified to investigate how the resting state EEG spectrum predicts behavioral performance (expressed as *cognitive processing speed ability*). Model 1 (Fig. 3C and D) estimated the latent level correlation between alpha oscillations and

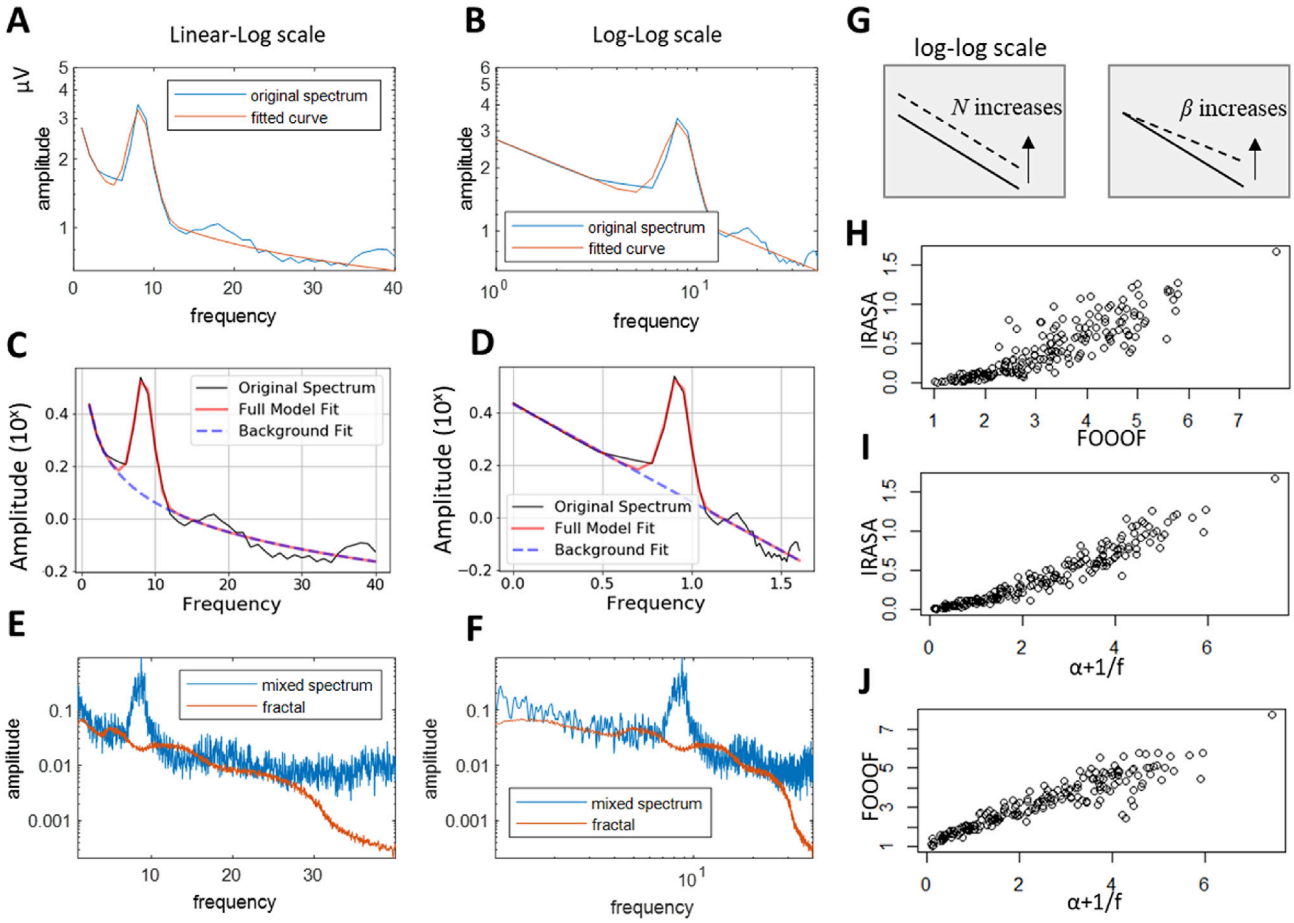

Fig. 2. Illustration of spectrum fitting based on different methods and the consistency among them. **A,B:** Original spectrum and its fitted curve for one participant based on 'α +1/f' method. The left one is in Linear (horizontal axis) – Log (vertical axis) scale. The right one is in Log-Log scale. **C,D:** Same results from FOOOF method. These two plots were generated by the FOOOF python toolbox. **E,F:** Same results from IRASA method. Note: As IRASA algorithm works on the entire time series rather than segment by segment, the frequency resolution is much higher, and consequently the amplitude scale is also different from the other two curve fitting methods. In this participant, the gamma range also appears to be deviated from the fractal component. **G:** Explanation of the meaning of *N* and *β* parameters. **H-J:** The scatter plots of estimated alpha amplitudes across participants from different methods served to demonstrate the consistency. The results are from eyes-closed condition.

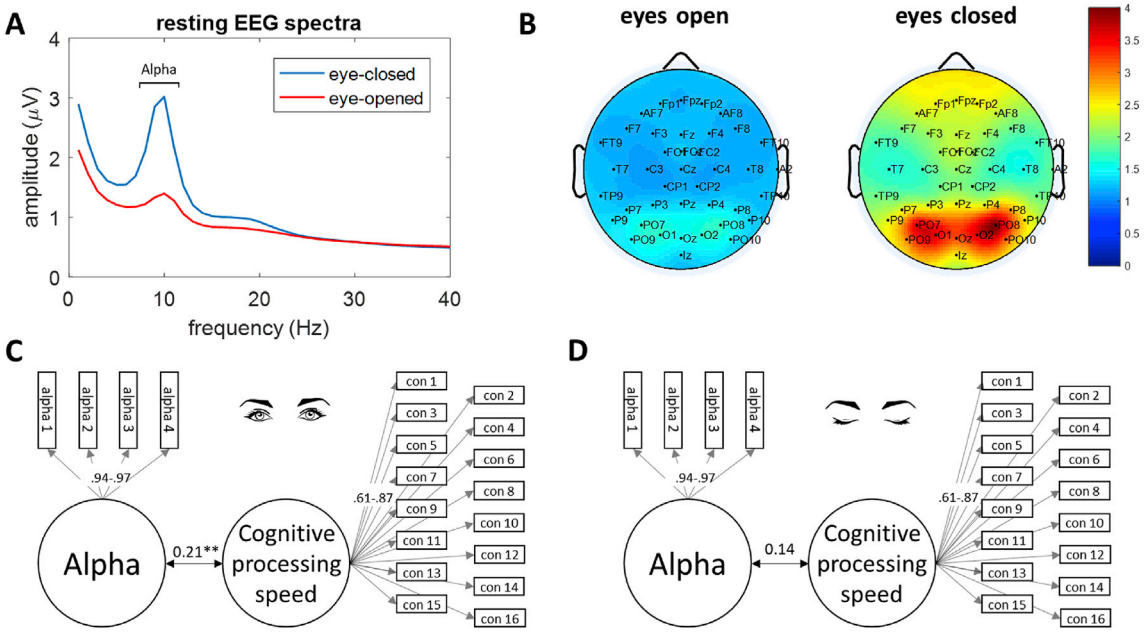

Fig. 3. Latent level correlation between overall alpha amplitude (8–12 Hz) and cognitive processing speed across participants. **A**: Spectra of resting-state EEG for both eyes-closed and eyes-open brain states. **B**: The topographies of alpha amplitude for both measurement states. **C, D**: Schematic representation of the SEMs correlating alpha and cognitive processing speed for both brain states. The correlations between the factors and the range of loadings are depicted in the diagrams. Model fit indices for the eyes-open state: CFI = 0.96, RMSEA = 0.09, for the eyes-closed state: CFI = 0.96, RMSEA = 0.10. For simplicity, the factors accounting for inter-individual variance due to experimental conditions (abbreviated as con in the figures, including the combination of two levels each for priming, familiarity, difficulty, and stimulus category) are not displayed. The models depicted in Panel C and D schematically follow the graphical language conventions of the SEM statistical literature: Rectagles represent measured variables, whereas circles are used to depict latent factors. Directed paths show factor loadings in our graphs and non-directed paths represent correlations at the level of latent variables.

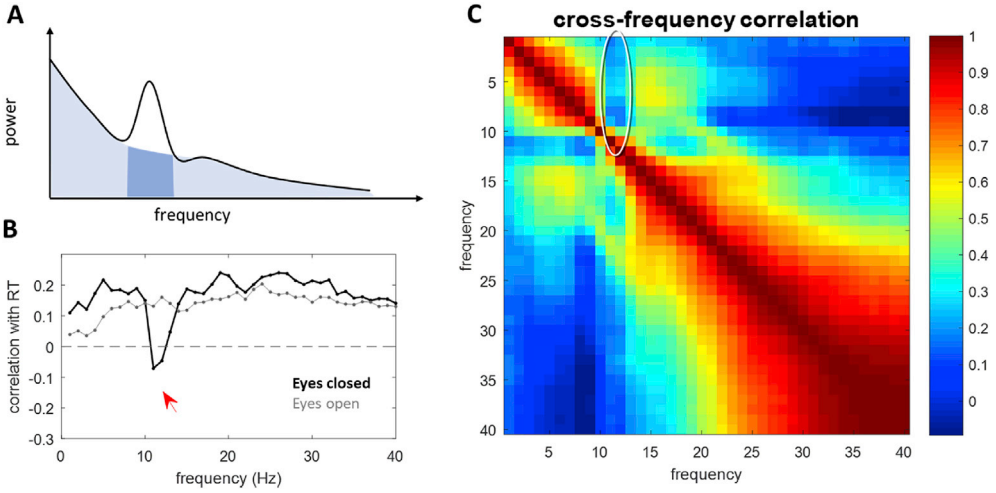

Fig. 4. Dichotomy between the alpha oscillation and the background 1/f noise in cross-individual amplitude variability. **A:** Illustration of the resting EEG spectrum. **B:** Correlation values between the signal amplitudes at different frequencies and average processing speed (RT) across participants. **C:** Cross-frequency correlations of the amplitudes of the oscillations across participants.

mean RTs across participants. Three type of factors were estimated in this model: an alpha factor (Alpha) based on the resting EEG data, a general factor of cognitive processing speed accounting for individual differences in mean response times across all task conditions, and specific factors nested below the general factor to account for the effects due to experimental manipulations (EX), i.e. difficulty, familiarity, priming, and stimulus category. More detailed information about this measurement model is provided in Fig. 3C and D. For simplicity, the EX factors are only displayed in the SI (Fig. S 1). In accordance with research conventions (Klimesch, 1999) and the features of the current data, alpha amplitude was sampled from within a frequency band ranging from 8 Hz to 12 Hz. For each participant, four segments were separately parameterized to serve as independent indicators in SEM. Each indicator was measured from the power spectrum averaged from a segment that was 10 s in length (see above section for power spectrum calculation). During EEG preprocessing, participants who did not have clean data (understood as such without abrupt jumping) longer than 40 s (yielding four indicators for psychometric modeling) were discarded from further SEM analyses. There were 194 participants left from the eyes-closed session and 200 participants from the eyes-open session. After merging the two EEG datasets with the behavioral RT data, 180 participants were left for SEM. For indicating how well the models fit the variance-covariance structure

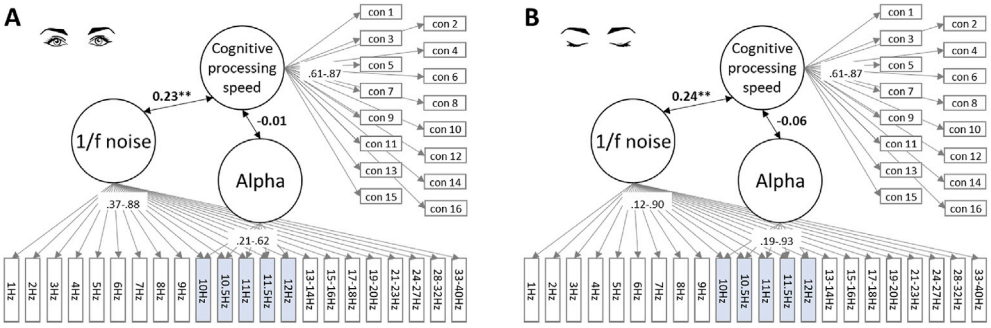

Fig. 5. Schematic, simplified SEM diagrams correlating 1/f noise and Alpha with cognitive processing speed. Model fit indices for the eyes-open condition: CFI = 0.93, RMSEA = 0.10, and for the eyes-closed condition: CFI = 0.93, RMSEA = 0.09. For simplicity, the factors accounting for experimental effects on RTs (priming, familiarity, difficulty, and stimulus category) are not displayed in these graphs (see the SI for the complete measurement model results for cognitive processing speed). The models depicted in Panel A and B schematically follow the graphical language conventions of the SEM statistical literature: Rectagles represent measured variables, whereas circles are used to depict latent factors. Directed paths show factor loadings in our graphs and non-directed paths represent correlations at the level of latent variables.

of the observed data, we report the Comparative Fit Index (CFI (Bentler, 1990), and the Root Mean Square Error of Approximation (RMSEA, (Steiger, 1980). SEM analysis was conducted by the *lavaan* package for R (Rosseel, 2012).

Model 2 estimated the latent level relationship between Alpha and cognitive processing speed versus 1/f noise and cognitive processing speed (Fig. 5). Four types of factors were modeled: Alpha, 1/f noise, cognitive processing speed, and specific factors capturing experimental manipulations. To create the indicators that we needed to model 1/f noise and Alpha factors, twenty-two indicators of frequency amplitude were sampled in the following way: 1 Hz, 2 Hz, 3 Hz, 4 Hz, 5 Hz, 6 Hz, 7 Hz, 8 Hz, 9 Hz, 10 Hz, 10.5 Hz, 11 Hz, 11.5 Hz, 12 Hz, 13–14 Hz, 15–16 Hz, 17–18 Hz, 19–20 Hz, 21–23 Hz, 24–27 Hz, 28–32 Hz, 33–40 Hz. The finer-grained sampling in the alpha band served the purpose of extracting the latent factor for a specific alpha amplitude. We selected the fine-grained range on the basis of the cross-frequency amplitude correlation matrix indicating the independence of the oscillations in the alpha range (Fig. 4). The spectrum indicators were modeled with two orthogonal latent factors, Alpha and 1/f noise (Fig. 5), both of which were allowed to be correlated with the general RT factor.

Model 3 (Fig. 6) estimated the latent level relationship between three power spectrum parameters along with their respective correlation with cognitive processing speed. The three parameters are the alpha amplitude (Alpha), the initial power law amplitude (N), and the power law exponent (β). These parameters were estimated by applying parametric fitting to the power spectrum, assuming that oscillatory and 1/f activity components contributed to the EEG spectrum. We applied three fitting algorithms for the purpose of examining the robustness of the main statistical results across algorithms used (see below for details). Again, for SEM analysis, each fitted parameter was obtained with four indicators from four equally divided data segments (each with a length of 10 s). The model is depicted in Fig. 6.

2.5. Estimation of alpha and 1/f parameters based on data fitting

2.5.1. Parametric curve fitting based on summation of the alpha bell function and the 1/f spectrum (α+1/f)

Following visual inspection of the power spectrum of the present data (Fig. 6E, G), we first developed a straightforward method that fit the spectrum of each participant between 1 and 40 Hz by the summation of a bell function (representing the alpha bump, see Fig. 3) and the power-law function (representing 1/f noise). For convenience, this method will be called 'α+1/f'.

The summation of the bell function and power-law function is:

$$D(x) = B(x) + P(x) = A\frac{1}{1-\left|\frac{x-c}{a}\right|^{b}}\mathrm{H}(x,c,w) + Nx^{-\beta}$$

where H is the Hann window function centered at c with width w, which constrains the left and right ends of the alpha bump to be strictly zero. There are five different parameters to be estimated: amplitude of alpha A, the center frequency of alpha c, the coverage width of the time window of alpha w (if alpha covers 8–12 Hz, w will be 5), the magnitude of the power law N and the power law exponent β (see Fig. 2G for the distinction between N and β). For simplicity, b is fixed to 1, and a is associated with w in a way that $a = w/4$ so that the bell shape properly covers the whole Hann window, and the width of the alpha bump can merely be estimated by w, which avoids redundancy in the two parameters (a and w) estimating the same feature.

The Parameter curve fitting is implemented by applying an iterative approach starting with initial values. The estimation of each parameter is confined in a plausible range (Table 1). Iteratively, the optimal value of each parameter corresponding to the minimum error function was identified and fixed before moving to the estimation of the next parameter. The iteration stops when all parameters have converged. The iteration usually converges after about 5 rounds, but up-to-50-iterations were allowed programmatically. When estimating the alpha-related parameters, the error function is defined as the least square error only confined around the alpha peak (c-2Hz, c-1Hz, c, c+1 Hz, c+2 Hz) because the other frequencies were irrelevant, and involving all the frequencies led to a very poor estimation of the alpha amplitude. When estimating the noise-related parameters (i.e., the power law), the error function involves all frequencies but is calculated in the log-log scale with L1-norm minimization to avoid outlier effects. In the log-log scale, the data were resampled with equal space ranging from left to right ends of the spectrum aiming to avoid a bias by the contribution of high frequencies to the data fitting. To this purpose the *interp1* function in Matlab was used. The estimation was conducted with an order of N -> β -> A -> c -> w. The initial values and confined realistic ranges are listed in Table 1. An example of fitting is shown in Fig. 2. The data and analysis scripts for this work can be obtained upon request.

	Initial value	Confined range	Meaning
A	2	[0, 10]	Amplitude of purified alpha
f	10	[7, 13]	Central frequency of alpha
w	5	[2, 10]	Width of alpha bump
N	left end of spectrum	–	Magnitude of power-law distribution
β	0.45	[0.2,0.8]	Exponent of power-law distribution

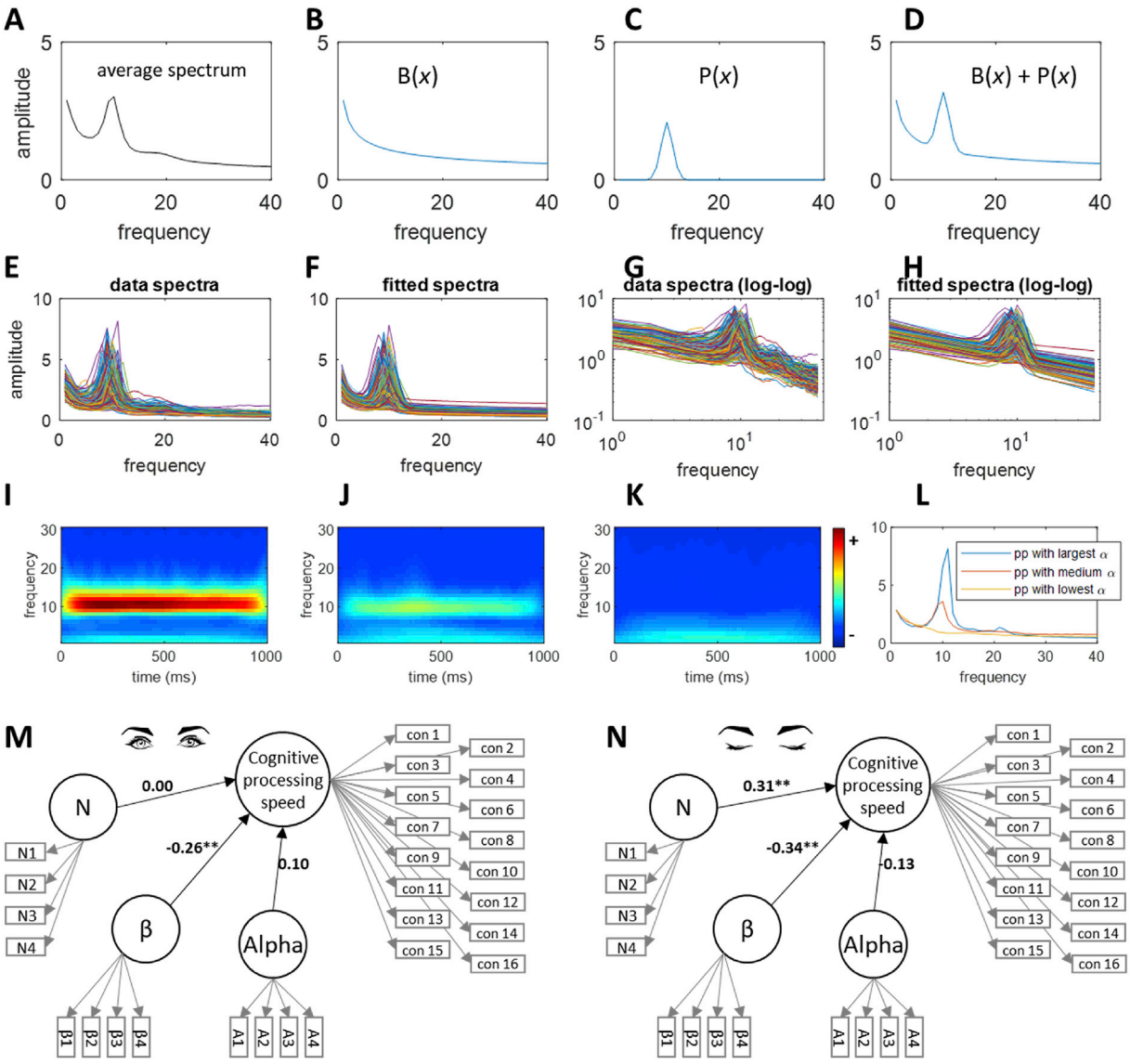

Fig. 6. Parameter fitting of the spectra and the relations of the fitted parameters with cognitive processing speed. **A**: spectrum pattern averaged across participants. **B-D**: illustrations of the bell function, power law function that was used by 'α+1/f' fitting method, and their summation. **E**: spectra for all participants. **F**: fitted spectra (by 'α+1/f' method) for all participants. **G, H**: same as E, F but given on a log-log scale. The data from A-H are from the eyes-closed state for purposes of illustration. **I, J, K**: The time-frequency pattern of three participants with the largest, medium, and smallest alpha amplitudes estimated by 'α+1/f' method as a demonstration of a valid parameter fitting. The wavelet analysis was applied to each 1-s segment of the data, and then the time frequency representation was averaged across segments. **L:** same participants as I–K but showing a Fourier spectrum. **M-N**: The SEM diagram relating the estimated alpha amplitude and the power law exponent with cognitive processing speed for both the eyes-open and eyes-closed conditions. The regression coefficients as shown in the diagram are from 'α+1/f' fitting method. The results for all three methods were summarized in Table 1. We allowed the predictors to be correlated (see below). Additionally, factors accounting for the effects of the experimental manipulations in the object processing task (priming, familiarity, difficulty, and stimulus category) on individual differences in observed RTs were estimated (see Fig. S 1), but they are not displayed here for simplicity (and because they are not relevant to the research questions we aimed to address). The models depicted in Panel M and N schematically follow the graphical language conventions of the SEM statistical literature: Rectagles represent measured variables, whereas circles are used to depict latent factors. Directed paths show factor loadings in our graphs and non-directed paths represent correlations at the level of latent variables.

Table 1
Regression coefficients of different spectrum parameters (N, β, Alpha) serving as independent (latent) variables in predicting cognitive processing speed ability.

	Eye open			Eye closed		
	N→Speed	β→Speed	Alpha→Speed	*N*→Speed	β→Speed	Alpha→Speed
α+1/f	-.00 (.993)	**-.26 (.003)**	.10 (.276)	**.31 (.004)**	**-.34 (.001)**	-.13 (.163)
FOOOF	.03 (.819)	**-.24 (.029)**	.15 (.135)	**.36 (.008)**	**-.41 (.002)**	-.04 (.702)
IRASA	.20 (.160)	**-.31 (.010)**	.00 (.998)	**.58 (.001)**	**-.40 (.003)**	-.21 (.097)

Note. *p*-values are indicated in parenthesis. Statistically significant relationships are highlighted in bold.

2.5.2. Fitting oscillations and one-over-f (FOOOF)

Although the above spectrum fitting algorithm that we propose (α+1/f) appears to capture the main features of the spectrum in our data as composed of alpha and 1/f components, there are limitations to it. The 'α+1/f' method relies on the assumption that a single dominant alpha oscillation exists in the data. While this presumption largely fits the visual pattern of the data at hand, there arguably exit some secondary narrowband, non-alpha oscillations spectrum, at least in some of the participants (Fig. 6). Such secondary non-alpha bumps can, in principle, affect the precision of estimating the 1/f parameters. Therefore, we further applied a more data-driven approach that fits the spectrum in a way that allows multiple oscillatory components, driven by specific spectrum pattern in individuals. FOOOF is a tool developed by Haller et al. (2018) for parameterizing neural power spectrum that was assumed to be the summation of 1/f and multiple narrowband oscillation humps. Aside from allowing different numbers of oscillation peaks in the spectrum, FOOOF adopted similar core principles of data fitting as our 'α+1/f' method, which is basically a parametric curve fitting. The alpha peaks in FOOOF is modeled as Gaussian function rather than a bell function. The objective function for the fitting is square error. In addition to the intercept (N) and slope parameter (β) of 1/f noise, FOOOF estimates the central frequency, bandwidth, and amplitude of each individual oscillation that was automatically detected. To avoid overfitting, we set the maximum of peaks to be three. The one that is closest to 11 Hz (center of alpha oscillation in the present data) was selected as the detected alpha and its amplitude was fed into subsequent SEM analysis for examining its relationships with behavior. The FOOOF toolbox is available on https://github.com/fooof-tools/fooof.

2.5.3. Irregular-resampling auto-spectral analysis (IRASA)

The parametric curve fitting approaches that were directly applied to fit the pattern of the power spectrum do not take into account how the power spectrum is generated. Thus, these approaches may have an inherent shortcoming in terms of misallocation of oscillation and 1/f component due to the so-called spectral leakage. Because of discretization, non-stationarity, damping, variations in central frequency over time, and multitude of oscillators, the peak of the central frequencies of oscillators may be blurred out to nearby frequency bands to different degrees. In terms of segregating the two different types of activity, the above mentioned factors may affect the performance of the fitting algorithms that directly fit curve functions to the spectrum pattern. This is why it is worthwhile to apply a decomposition method that is oriented to the defining nature of the components, rather than their appearance in the end-product of the spectrum. The method IRASA (Wen and Liu, 2016b) was particularly developed for this purpose. Specifically, IRASA rests upon the definitions of 1/f and oscillation such that the power spectrum calculated from resampled (either up or down sample) time series of 1/f activity will remain the same as from the original data, whereas the spectrum from the resampled activity of an oscillation will systematically shift the peak frequency at the scale of resampling (Wen and Liu, 2016b). Based on this principle, the IRASA algorithm separates the spectrum of oscillatory and 1/f (called fractal in the original paper) activities.

We applied IRASA to our present data using the four different segments that serve as four indicators (using original rescale factor 1.1 to 1.9 with a space of 0.1). IRASA is not exactly a data fitting method. After the decomposition of oscillation and 1/f spectrum, we quantified the intercept N, slope β from the linear regression parameters of the IRASA-decomposed fractal spectrum. The alpha amplitude was simply calculated from the amplitude between 8 and 12 Hz from the IRASA-decomposed oscillation spectrum.

In summary, we applied the above described three algorithms to quantify the alpha amplitude (A), intercept and slope of the 1/f spectrum, N and β with three different approaches proposed in the literature. This will allow us to examine the robustness of the investigated relationships with cognitive processing speed across analysis algorithms. The fitting results based on each method from one participant was shown in Fig. 2(A–E) to illustrate the general principle. The consistency among them are relatively high as showed by high correlation in the estimated alpha amplitude from different methods (Fig. 2H–J).

3. Results

3.1. Estimating a latent variable reflecting cognitive processing speed

In the present study, we focused on processing speed as a proxy for cognitive processing efficiency. Cognitive processing speed is conceptualized as a latent variable that accounts for covariation in individuals' reaction times (RT) captured across basic cognitive tasks. It is thus extracted from participants' RT data on perceptual decision tasks administered with multiple experimental conditions (see the Methods section for details). Specifically, hierarchically nested factor analyses were used to statistically dissociate a cognitive processing speed factor from condition-specific latent factors that capture condition-induced components of variance (e.g., specific individual differences due to differential effects of priming, familiarity, difficulty, and stimulus category). Thereby, the estimated measurement model comprised five factors: A general factor (termed cognitive processing speed) and four orthogonal factors capturing the individual differences that were due to the experimental manipulations (see Fig. S1). This measurement model revealed a satisfactory fit to the data: All factor loadings were substantial and significant (see Fig. S1), and the model fit indexes were CFI = 0.95, RMSEA = 0.13. Thus, the extracted general factor serves as a suitable latent ability estimate of between-person differences in cognitive processing speed that can be predicted by EEG spectrum measures.

3.2. Estimating latent level correlations between alpha amplitude and cognitive processing speed

The resting state EEG spectrum showed a clear alpha peak in both measurement states (eyes closed and eyes open, Fig. 3 A) with a commonly observed occipital distribution (Fig. 3 B). Alpha amplitude and cognitive processing speed were modeled as two correlated latent factors (named Alpha and cognitive processing speed, Fig. 3C and D). The isolated modeling of the two measurement states was necessary because a previously estimated model revealed that separate alpha amplitude factors accounted for between-person variability in the two resting EEG states (see Fig. S4). A significant correlation between Alpha and cognitive processing speed was found in the eyes-open state only, even though the alpha oscillation was two times stronger in the eyes-closed state than in the eyes-open state (Fig. 3 A). This finding appears puzzling because a larger magnitude of alpha is commonly associated with a higher signal-to-noise ratio of the alpha band and thus the more reliable measurement of alpha within individuals. We thus further asked about the extent to which the Alpha-Speed correlation was actually driven by Alpha (Alpha is capitalized when it refers to the factor). The following analyses were designed to figure out this puzzle.

3.3. Dissociating alpha oscillation from 1/f noise

We hypothesized that the variation in alpha amplitude across participants measured from the raw data would be generated to a considerable degree by the background 1/f noise within the alpha band (depicted as a dark blue area underlying the alpha peak in Fig. 4 A). We will refer to this as the 1/f portion of alpha (shortened to 1/f alpha). In a similar vein, we refer to the portion of alpha above the 1/f curve as the purified alpha. 1/f alpha belongs to the continuum of 1/f noise and, thus, does not have an oscillatory nature. Therefore, we hypothesized that the purified alpha and the 1/f alpha are dissociable in terms of their amplitude variability across persons. Furthermore, we hypothesized that the Alpha-Speed correlation as estimated on the basis of the raw EEG data would mainly be driven by the 1/f portion of alpha. If this was the case, a

stronger purified alpha would lead to lower Alpha-Speed correlations, thus explaining the result in Fig. 3C and D.

Furthermore, if our assumptions about the 1/f alpha-speed correlation are correct, it should not just hold in the alpha band. This is because the alpha band is not unique in the spectrum of 1/f noise. It is more likely that the continuum of the 1/f spectrum (Fig. 4 A, both light and dark blue areas) is globally (i.e., broadband) associated with cognitive processing speed. We first tested this hypothesis by simply correlating the amplitude in every frequency with the observed average processing speed across participants (Fig. 4 B). The correlations turned out to be positive for all frequencies, suggesting a broadband relationship. Remarkably, an abrupt drop appeared in the alpha band for the eyes-closed measurement state (Fig. 4 B), going along with the functional dichotomy between alpha and broadband 1/f noise.

To further demonstrate the dichotomy between the alpha oscillation and the broadband 1/f noise, we plotted the cross-frequency correlation matrix in Fig. 4 C. Specifically, we calculated the correlations for the oscillation amplitudes across participants between every pair of frequencies from 1 to 40 Hz. Presumably, the correlations would decay with the distance between the pair of frequencies, i.e., nearby frequencies would be more strongly correlated, whereas distant frequencies would be less strongly correlated. It turned out that this was the case in general, but not for alpha oscillations that were not correlated with both nearby and distant frequencies (Fig. 4 C, indicated with the white ellipse).

The multifaceted evidence summarized above suggests that the alpha oscillations are largely dissociable from the background 1/f fluctuations in terms of between-person variability and their associations with behavioral performance. Such mixed inter-individual variability seems ideally suited for structural equation modeling (SEM), which is summarized in the next section.

3.4. Estimating latent level correlations of purified alpha and 1/f noise with cognitive processing speed

Building on the descriptive evidence presented above, we modeled two orthogonal latent factors that could explain the covariances of the amplitudes at different frequencies across participants: alpha and 1/f noise. The 1/f noise refers to the broadband activity with a 1/f-like pattern. To be precise, the term "1/f" only carries the indication that the power is inversely proportional to the frequency. More precise mathematical forms depicting this broadband EEG activity have been studied elsewhere (He, 2014; He et al., 2010b). The Alpha factor accounts for between-person variability in the amplitude of pure alpha oscillations. The 1/f noise factor accounts for between-person variability in the magnitude of the broadband EEG activity. On the basis of the assumptions summarized above, we expected the following with respect to the relationships between the Alpha, 1/f noise, and cognitive processing speed factors: 1) Stronger 1/f noise should be associated with slower performance, for both eyes-closed and eyes-open states; 2) Individual differences in alpha oscillation power should not be associated with cognitive processing speed. These assumptions were fully corroborated by the SEMs illustrated schematically in Fig. 5. Please note that we correlated the Alpha and 1/f noise factors with the cognitive processing speed factor for the eyes-open and eyes-closed states separately because the measurement model revealed specific individual differences between the two measurement states (see Fig. S5 in the SI).

Although mean RTs have been commonly used as an indicator of cognitive performance (here, cognitive processing speed), there are some other ways to characterize cognitive performance with RT data. In addition to the results based on mean RTs as provided in Fig. 5, we also examined the latent correlations between the resting EEG features (1/f noise, alpha) and other methods of behavioral characterization. A popular description of RT distributions is the ex-Gaussian model, which describes the distribution with three parameters—μ, σ, and τ—corresponding to the central peak, the width, and the skewness of the distribution, respectively. Conceptually, μ represents the central speed, σ represents the variability, and τ represents the tendency to give overly slow responses or outliers. We used a two-step maximum likelihood procedure to estimate the three ex-Gaussian parameters (Massidda, 2013; Van Zandt, 2000), and we analyzed their relationships with both the 1/f noise and Alpha factors in the SEM framework (Fig. 5). The results showed that the 1/f noise-Speed correlation was more strongly manifested in the τ parameter: In the eyes-open condition, r(1/f noise, μ) = 0.17, p = .034, r(1/f noise, σ) = 0.19, p = .38, r(1/f noise, τ) = 0.31, p < .001; In the eyes-closed condition, r(1/f noise, μ) = 0.21, p = .01, r(1/f noise, σ) = 0.16, p = .069, r(1/f noise, τ) = 0.28, p = .003. The Alpha factor remained consistently uncorrelated with all ex-Gaussian parameters. The three ex-Gaussian parameters were highly intercorrelated: r(μ, σ) = 0.78, p < .001; r(μ, τ) = 0.32, p < .001; r(σ, τ) = 0.66, p < .001.

3.5. Which property of the 1/f noise factor predicts cognitive processing speed?

The SEM results described above revealed that the between-person variance in cognitive processing speed could be significantly explained by variability in the magnitude of 1/f noise but not by the alpha oscillations. This correlational relationship is informative in terms of individual differences; however, it barely provides any information about the possible functional mechanism that is supported by the broadband activity. A more profound understanding of the functional mechanism requires a dissecting of the relationship between the 1/f noise and cognitive processing speed with respect to specific properties of the 1/f spectrum. For instance, the pattern of the 1/f spectrum may vary across individuals in baseline level or rate of decay (Voytek and Knight, 2015), each of which could contribute to the relationship with cognitive processing speed, but different dynamic mechanisms may underlie the different associations. To address this question, we further conducted data fitting approaches to estimate the key parameters that characterize the 1/f spectrum and correlated the fitted parameters with behavior in the SEM models.

A visual inspection of the spectrum pattern in Fig. 3 suggests that the spectrum is mainly composed of broadband component and a protruding bump of alpha oscillation. The broadband can be formulated by the power law function $P(x) = Nx^{-\beta}$, which is a feature that has been claimed to reflect the intrinsic nature of self-organized criticality of complex dynamic systems (Bak et al., 1987; Hesse and Gross, 2014). Here, x denotes the frequency, β denotes the power law exponent, and N is the initial amplitude. A smaller β corresponds to a spectrum pattern that is closer to a white noise pattern – the most irregular time series with a zero auto-correlation. With respect to the oscillation component, although the grand average spectrum (Fig. 3) displays a clearly shaped oscillation at alpha band, at individual level, the morphology of this alpha peak could be variable (thus, multiple peaks could exist). We applied three methods to estimate the amplitude of the alpha oscillation at the individual level (see Method description above) and denote it as A. In sum, there are three parameters: A (purified alpha amplitude), β (power law exponent), and N (initial amplitude of the power-law) that were estimated and were related to cognitive processing speed in a manner similar to the one depicted in Fig. 5.

Given the dichotomy of the curve-fitting parameters between the eyes-open and eyes-closed states (see Fig. S 6), we analyzed the relationship between the estimated spectrum parameters and cognitive processing speed in two separate SEMs – for eyes-open and eyes-closed separately. The results summarized in Fig. 6 describing the relationships between spectrum parameters and cognitive processing speed were derived from 'α+1/f' method. The results derived from the other two methods are reported in Table 1 and show high consistency. We can see that the power law exponent predicted cognitive processing speed in the sense that larger average speed went along with smaller β values (stronger decay). The power law amplitude N also predicted processing speed but only in the eyes-closed condition. The estimated alpha

amplitudes were again not predictive of cognitive processing speed, thus confirming the absence of a consistent relationship between purified alpha oscillations and cognitive processing efficiency. Although not shown in Fig. 6, between-person correlations between different spectrum parameters existed: For the eyes-open state, $r(N, \beta) = 0.23$, $p = .002$, $r(\text{Alpha}, \beta) = -0.04$, $p = .60$; $r(\text{Alpha}, N) = 0.47$, $p < .001$; and for the eyes-closed state, $r(N, \beta) = 0.48$, $p < .001$, $r(\text{Alpha}, \beta) = -0.21$, $p = .006$, $r(\text{Alpha}, N) = 0.29$, $p < .001$.

Table 1 illustrates the results on the relationships between the latent factors of the three key spectrum parameters and the latent factor of cognitive processing speed from all applied fitting methods. In brief, the parameters of 1/f noise are consistently predicting speed whereas the alpha amplitude does not. Detailed SEM results from all three methods are reported in SI.

4. Discussion

4.1. Summary

The present study aimed at investigating how individual differences in a basic cognitive ability (cognitive processing speed) could be predicted by the power spectrum of resting-state EEG signals. Previous research on EEG spectrum analysis has repeatedly reported correlations between cognitive performance and oscillatory brain activity in various frequency bands, particularly alpha (Ergenoglu et al., 2004; Haegens et al., 2010; Lange et al., 2012; Linkenkaer-Hansen et al., 2004; Van Dijk et al., 2008; Weisz et al., 2014; Zhang and Ding, 2010). However, the broadband, non-oscillatory 1/f noise-like brain activity, that are confounded with alpha oscillations in the spectrum, are also functionally relevant *per se* (Bassettt et al., 2006; Colombo et al., 2019; Dave et al., 2018; He, 2014; Palva et al., 2013; Podvalny et al., 2015; Tagliazucchi et al., 2013; Voytek et al., 2015; Waschke et al., 2017). Therefore, we attempted to investigate how these two major kinds of ongoing brain activities are differentially associated with cognitive ability, for which we needed to dissociate the oscillatory and non-oscillatory brain activities. This is because the oscillatory components can be substantially confounded with the predominant activity of 1/f noise. With structural equation modeling, we differentiated the sources of variability from the resting EEG signal that were differentially correlated with cognitive processing speed. The SEM analysis revealed a dichotomy of the 1/f noise component versus the purified alpha oscillation in terms of cross-person variability. The dissociation further revealed that the alpha oscillations, which are the predominant brain oscillations that show a peak at around 10 Hz, did not show a significant association with cognitive processing speed after individual differences in the 1/f noise were partialed out by means of SEM. This was the case even though a significant alpha-behavior association was observed in the analysis of the raw data, i.e., without removing the 1/f portion of alpha. Variability in the 1/f noise was revealed by SEM to robustly predict cognitive processing speed in both the eyes-open and eyes-closed measurement states. In addition to SEM-based analysis, we applied three different data-analytic strategies of parameter estimation at the level of the individual data to further investigate which aspect of 1/f spectrum predicts cognitive ability. The different fitting methods consistently revealed that the slope of the power-law decaying function predicted between-person variability in cognitive processing speed, analyzed here as a proxy for basic cognitive performance.

4.2. Current issues in EEG spectrum analysis and solutions

The scalp EEG signal has been canonically classified into five frequency bands: delta: <3 Hz; theta: 4–7 Hz; alpha: 8–12 Hz; beta: 13–30 Hz; gamma: >30 Hz. Although a number of studies have discovered EEG oscillation patterns that display defining frequency bands that fall into these specific bands (Cavanagh and Frank, 2014; Klimesch et al., 2007; Tallon-Baudry and Bertrand, 1999), the rationale behind the above categorization in terms of functional specificity with respect to the underlying neural generators has not yet been soundly established (Buzsaki et al., 2013). More importantly, the genuineness of oscillations circumvented by a narrow band has been debated (Buzsaki, 2006). The EEG spectrum was shown to display 1/f-like patterns that are typically observed in signals generated by complex systems (Freeman et al., 2003; Markovic and Gros, 2014; Miller et al., 2009; Pritchard, 1992). From the perspective of complex systems, the power-law pattern is an intrinsic property of complex dynamic systems with a self-organized order that differentiates these systems from randomness (Markovic and Gros, 2014). Therefore, it seems inappropriate to analyze the 1/f continuum in a narrowband fashion. This is because the 1/f pattern, as a holistic feature, penetrates the entire EEG spectrum. The brain oscillation as defined in the conventional way – a narrow band taken from the entire 1/f spectrum – may be conceptually elusive. For instance, the power of infra-slow or delta oscillation (<3 Hz) is largely contributed by the 1/f component, despite the fact that a genuine oscillation pattern might exist (Demanuele et al., 2007). Given that a large body of EEG analyses in frequency domain have been based on power analysis on the raw spectrum, we advocate shifting the spectrum analysis from a band-based power calculation to a more sophisticated approach that dissects the spectrum into overlapping oscillatory and non-oscillatory components appears to be indicated. In fact, the mixture issue has been recognized and a number of methods have been developed and applied to address this problem, with different levels of sophistication, e.g., whitening the spectrum by removing the linear component in the log-log scale (Buzsaki, 2006), or removing the across-condition average spectrum (Demanuele et al., 2007), or purely data-driven approaches that involve modeling the spectrum pattern (Haller et al., 2018), or simply removing the average of the left and right ends of the alpha bump when analyzing alpha power (Parameshwaran and Thiagarajan, 2017). Notably, there are methods (also applied in the present work) that have been developed to segregate the oscillatory and 1/f component based on algorithms that utilized their defining features in the time series (Wen and Liu, 2016b; Yamamoto and Hughson, 1993), rather than on their different manifestations in the spectrum. These methods could be applied to isolate the 1/f component from the oscillatory activities before the narrowband-oriented analysis (e.g., investigating the functional roles of alpha). In the present work, we introduced a novel solution for spectrum decomposition: structural equation modeling. The SEM method explicitly utilized the between-person variability as the basis for factorizing and decomposing (Model 2) alpha and 1/f, based on which differential relationships with cognitive ability could be demonstrated. Method comparisons are discussed below, but the converging results about the spectrum-behavior relationships from the various methods with very diverse theoretical basis strongly substantiated the necessity of decomposing the spectrum when studying the neural basis of cognitive performance.

4.3. How can the present findings inspire research on brain oscillations?

Oscillations are a prominent feature of neural dynamics and are undoubtedly a crucial reflection of neural working mechanisms. Owing to their importance and ubiquity, a large body of neuroscience research has focused on neural oscillations. The EEG alpha oscillations have been studied for more than one century (Berger, 1929). In contrast, the non-oscillatory, 1/f noise-like activity used to be deemed unimportant and only started to receive attention in recent years (He, 2014). Therefore, a large body of brain activity analysis in the frequency domain, including many contemporary works, did not consider the effect contributed by 1/f. A main contribution of our work is that, we have demonstrated the necessity of disentangling them when investigating EEG spectrum-cognition relationships. Without disentangling the two, the obtained relationships could strongly diversify the view on neural oscillations across specific research contexts. In the present case, after the disentanglement that was based on the SEM approach, the prominent EEG alpha oscillations do not seem to play a key functional role in

explaining cognitive performance (here, cognitive processing speed) as measured with a traditional stimulus familiarity decision task, whereas the background 1/f noise does. Without separating alpha from the non-oscillatory part of the signal, alpha would be mistaken as the neural account of between-person differences in the present cognitive performance data. This clear disparity in conclusions about the functional role of brain oscillations speaks to the necessity to their dissociation in future work. In a broader sense, the entanglement of oscillations and 1/f noise could lead to both Type I and Type II errors concerning the association between oscillation and cognition. Both are possible when researchers examine a variety of other cognitive domains. It is conceivable that the dissociation of oscillations and 1/f noise in signal processing may lead to an even stronger functional association between oscillation and behavior if the functionally responsible component is the oscillation but not 1/f noise.

4.4. Is "1/f noise" really noise?

When interpreting the present findings, we need to clarify the use of the terminology "1/f noise" in many places. Identifying this component as "noise" may be conceptually confusing (although commonly used). The term "noise" usually refers to something irregular, unexplained, and functionally irrelevant. However, in neurobiological systems, the role of noise is complex in the sense that its existence has been claimed to be functionally beneficial and necessary (McDonnell and Ward, 2011). Although its mechanism is not fully understood (the generative mechanisms can be diverse, see He, 2014), the functional relevance of the specific patterns of 1/f noise has been widely demonstrated (Bassettt et al., 2006; He, 2014; Palva et al., 2013; Tagliazucchi et al., 2013; Voytek et al., 2015). Notably, the power law scaling has been found to be strongly modulated by brain activation during task processing (Podvalny et al., 2015). Moreover, the power law scaling was significantly correlated with brain oscillations from moment to moment, and was very sensitive to pharmacological interventions (Muthukumaraswamy and Liley, 2018). Such concrete evidence revealed that the 1/f activity is closely engaged in both cognitive processing and maintenance of brain functions – 1/f activity is not only more than noise; it encodes fundamental function. This explains our results indicating the 1/f parameters to be correlated with general cognitive processing speed extracted from the RT indicators of all task conditions, but not with any task condition-related variability.

In this regard, the 1/f "noise" as we called it here can be regarded as the broadband brain activity that is clearly functionally relevant. How those signals are generated by neural circuits and systems, and why they appear in this form represent questions to be addressed in future work to gain further understanding of individual differences in cognitive ability from a mechanistic point of view. By studying the generative model of 1/f we could pinpoint to the key parameters, processes, or configurations that are responsible for alternation of 1/f features. For example, the excitation-inhibition (E-I) balance of neural circuits alters the slope of power law spectrum, and computational neural circuit model have been developed to resemble this process, thus allowing inference of E-I balance from neurophysiological signals (Gao et al., 2017). Regarding the generative models that have been proposed, one popular theory intended to explain the genesis of power law phenomena is the so called self-organized criticality (SOC) theory (Bak et al., 1987; Beggs, 2008; Beggs and Plenz, 2003; Hesse and Gross, 2014). SOC posits that the power law feature is an emerging phenomenon that originates from interacting dynamical systems that run in critical states, which is optimal for information processing (Beggs, 2008). Sub-optimal functioning, including pathological states, would appear on the dynamical regime that deviates from critical states (Meisel et al., 2012). However, it has to be noted that several alternative mechanisms for generating power law feature have been proposed, for examples, intrinsic low-pass filtering of neural current by dendritic structure (Linden et al., 2010), frequency dependence of current propagation in biological tissue (Bedard and Destexhe, 2009), or mixture of damped neural oscillators having a distribution of relaxation rates (Muthukumaraswamy and Liley, 2018). These models provide testable mechanisms by which the 1/f pattern may be generated, and its associations with functional processing may be supported.

Our results revealed that the 1/f noise, the continuum in the spectrum, appears to be an entity that is predictive of individual differences in cognitive ability. At first glance, this relationship would mean that the stronger the broadband activity of a participant, the slower would be the participant's response speed. One possible interpretation is that a stronger baseline of neural activity, and thus brain metabolism, leads to sub-optimal basic cognitive function. This interpretation would need further systematic testing because the overall strength of an EEG signal measured from the scalp could be due to many more factors other than brain metabolism, for example, the conductivity of scalp, skull, and inner tissues (Klimesch, 1999). We further investigated whether the behavioral variability is due to the detailed structure of the 1/f pattern rather than simply the magnitude. For that we conducted different data fitting analysis on the spectrum pattern. The results consistently revealed that the smaller delaying (closer to white noise) parameter of the 1/f pattern mainly accounted for cognitive slowing. This demonstrated that the inner structure of the 1/f pattern reflects important properties of brain physiology and the neural network system, which may provide new source of experiment data for testing various models of 1/f signal genesis.

4.5. What does the performance measure reflect?

In this work, we used average reaction times as a simple indicator of cognitive performance. This is arguably a straightforward indicator of cognitive processing speed, which reflects a very fundamental property of brain functioning. However, the limitations of using average reaction times to represent processing efficiency have been raised (Heathcote et al., 1991; Larson and Alderton, 1990; Luce, 1986). The major drawback of such an approach is that the mean reaction time does not reflect a unitary feature of cognitive performance but rather a mixture of multiple different features. Specifically, a person's behavior pattern is fully encoded in the whole distribution of single-trial reaction times, which are composed of multiple parameters depending on the proposed models. The ex-Gaussian is a popular description of reaction time distributions; it describes the distribution with three parameters—μ, σ, and τ—which correspond to the central peak, the width, and the skewness of the distribution, respectively. In behavioral studies using the ex-Gaussian reaction time decomposition, τ has been consistently shown to be better at predicting higher order cognitive abilities (e.g., working memory capacity and fluid intelligence) in comparison with μ (Schmiedek et al., 2007; Schmitz and Wilhelm, 2016; Unsworth et al., 2010).

It was therefore interesting to investigate which aspect of the RT distribution would be found to be critically associated with the resting-state EEG spectrum, specifically, the 1/f noise factor. Our analysis showed that the 1/f noise-speed correlation was more strongly manifested in the τ parameter in both the eyes-open and eyes-closed states. The alpha factor remained consistently uncorrelated with all ex-Gaussian parameters. Thus, the 1/f noise factor was more strongly associated with the τ parameter in comparison with the mean RT, although the improvement was only moderate. The results showed that the three ex-Gaussian parameters were highly intercorrelated. Therefore, we could not conclude that the 1/f noise factor was exclusively associated with the skewness of the RT distribution.

4.6. How SEM and the parametric curve fitting approach compare in parameterizing the noise component

To dissociate the 1/f part of the EEG spectrum that was qualitatively distinct from the alpha bump, we employed two different types of approaches: between-person decomposition by using an SEM approach and within-person parameter estimation. In the SEM approach, we first

parameterized the amplitude of the spectrum at every frequency and assigned two orthogonal factors that captured the variability of the within-alpha frequencies and all frequencies (representing the background noise). This variance decomposition approach is based on the conceptual assumption that there exist two factors that distinctively capture between-person variability in alpha oscillation and 1/f activity. The portion of frequency power within the alpha band that does not belong to oscillations (the dark blue area in Fig. 4) will then be captured by the 1/f noise factor because it covaries with the overall 1/f noise strength across participants.

On the contrary, individual-data-based estimation of the spectrum parameters is solely based on the descriptive features of individual spectrum pattern, which is mainly composed of an alpha bump and a power-law curve. Both approaches have advantages and disadvantages. The SEM approach explicitly utilizes between-person variability as its foundation in order to dissociate the two factors. This would boost the relevance of the factors we expected to capture, namely, individual differences in the alpha oscillations and the 1/f part. However, it lacks the consideration of specificity within individuals, e.g., peak alpha frequencies. The individual parameterization approach is better suited for capturing the specificities in individual participants, but it may, on the other hand, suffer from such specificities. For example, the power law pattern has shown relatively large variability across participants. The overall pattern tends to display a power-law shape, but for specific individuals, the pattern may deviate substantially from a power-law shape, thus rendering the estimation less reliable. Moreover, studies found that neurophysiological activities appear to be composed of different power law components with different slopes, and determining of the knee point still remains an open question (He et al., 2010a; Muthukumaraswamy and Liley, 2018; Wen and Liu, 2016a). Thus, the parametric curve fitting methods that were used in the individual-data-based approach may have the limitation that the spectral components may not perfectly fit the assumed parametric functions at the individual level.

The purpose of applying two very different approaches to model alpha and 1/f noise is to demonstrate that their respective correlations with behavior are consistent across different data-analysis strategies. Both approaches revealed that the real alpha oscillation is not correlated with cognitive processing speed, whereas the background 1/f noise is consistently correlated with it. From a methodological perspective, we demonstrated the robustness of these postulated relationships by the convergent conclusions that came from different analysis approaches. Such a convergence additionally supported the idea that in future research on EEG oscillations and cognition, the 1/f component needs to be fully accounted for.

4.7. Spatial feature of the 1/f-behavior relationship

Finally, we discuss the spatial specificity of the 1/f-behavior relationship. Unlike alpha oscillations, which show a specific localized scalp distribution at occipital areas, the 1/f pattern is a universal feature that appears to be more broadly spread across space (He et al., 2010b; Muthukumaraswamy and Liley, 2018). The correlation between power law scaling and other physiological or behavioral factors were found to be either spread or localized, but without a consistent pattern across studies (Dave et al., 2018; Muthukumaraswamy and Liley, 2018; Voytek et al., 2015). Our current 1/f and cognitive speed relationship did not show a clear spatial structure: We conducted the SEM analysis as done in Fig. 5 separately on each electrode and plotted the distribution of the 1/f-RT latent correlation across the scalp, the results did not seem to show a specific distribution that was consistent across eye states (Fig. S 7). More importantly, the pattern did not resemble the scalp pattern for alpha (Fig. 3) at all, again confirming its difference from alpha oscillations. The lack of spatial specificity in the present study may imply that the functional characteristic of 1/f activity is largely global, but it could also be due to insufficient spatial resolution of EEG measurement. The spatial pattern of such 1/f and cognitive behavior relationship may be rather investigated with a neuroimaging approach characterized by higher spatial resolution (e.g., high density EEG, fMRI), which is a relevant topic for future research.

Funding

This work was partially supported by Hong Kong Research Grant Council (ECS 27603818) and the Seed Fund for Basic Research from the University of Hong Kong (No. 201804159003) to GO, and by the Deutsche Forschungsgemeinschaft (HI 1780/2-1) to AH and Werner Sommer (SO 177126-1), and by the Deutsche Forschungsgemeinschaft (SCHM 3235/3-1) to FS and Oliver Wilhelm, and by the German Federal Ministry of Education and Research (BMBF, 13GW0273D) to CSH.

Appendix A. Supplementary data

Supplementary data to this article can be found online at https://doi.org/10.1016/j.neuroimage.2019.116304.

References

Arnal, L.H., Giraud, A.L., 2012. Cortical oscillations and sensory predictions. Trends Cogn. Sci. 16, 390–398.
Babu Henry Samuel, I., Wang, C., Hu, Z., Ding, M., 2018. The frequency of alpha oscillations: task-dependent modulation and its functional significance. Neuroimage 183, 897–906.
Bak, P., Tang, C., Wiesenfeld, K., 1987. Self-organized criticality - an explanation of 1/F noise. Phys. Rev. Lett. 59, 381–384.
Basar, E., 2012. A review of alpha activity in integrative brain function: fundamental physiology, sensory coding, cognition and pathology. Int. J. Psychophysiol. 86, 1–24.
Bassettt, D.S., Meyer-Lindenberg, A., Achard, S., Duke, T., Bullmore, E.T., 2006. Adaptive reconfiguration of fractal small-world human brain functional networks. Proc. Natl. Acad. Sci. U.S.A. 103, 19518–19523.
Bauml, K.H., Hanslmayr, S., Pastotter, B., Klimesch, W., 2008. Oscillatory correlates of intentional updating in episodic memory. Neuroimage 41, 596–604.
Bedard, C., Destexhe, A., 2009. Macroscopic models of local field potentials and the apparent 1/f noise in brain activity. Biophys. J. 96, 2589–2603.
Beggs, J.M., 2008. The criticality hypothesis: how local cortical networks might optimize information processing. Philos. Trans. R. Soc. A Math. Phys. Eng. Sci. 366, 329–343.
Beggs, J.M., Plenz, D., 2003. Neuronal avalanches in neocortical circuits. J. Neurosci. 23, 11167–11177.
Bentler, P.M., 1990. Comparative fit indexes in structural models. Psychol. Bull. 107, 238–246.
Berger, H., 1929. Über das elektrenkephalogramm des menschen. Eur. Arch. Psychiatry Clin. Neurosci. 87, 527–570.
Bullock, T.H., McClune, M.C., Enright, J.T., 2003. Are the electroencephalograms mainly rhythmic? Assessment of periodicity in wide-band time series. Neuroscience 121, 233–252.
Buzsaki, G., 2006. Rhythms of the Brain. Oxford University Press.
Buzsaki, G., Logothetis, N., Singer, W., 2013. Scaling brain size, keeping timing: evolutionary preservation of brain rhythms. Neuron 80, 751–764.
Cavanagh, J.F., Frank, M.J., 2014. Frontal theta as a mechanism for cognitive control. Trends Cogn. Sci. 18, 414–421.
Chaumon, M., Bishop, D.V., Busch, N.A., 2015. A practical guide to the selection of independent components of the electroencephalogram for artifact correction. J. Neurosci. Methods 250, 47–63.
Colombo, M.A., Napolitani, M., Boly, M., Gosseries, O., Casarotto, S., Rosanova, M., Brichant, J.-F., Boveroux, P., Rex, S., Laureys, S., 2019. The spectral exponent of the resting EEG indexes the presence of consciousness during unresponsiveness induced by propofol, xenon, and ketamine. Neuroimage 189, 631–644.
Dave, S., Brothers, T.A., Swaab, T.Y., 2018. 1/f neural noise and electrophysiological indices of contextual prediction in aging. Brain Res. 1691, 34–43.
Delorme, A., Makeig, S., 2004. EEGLAB: an open source toolbox for analysis of single-trial EEG dynamics including independent component analysis. J. Neurosci. Methods 134, 9–21.
Demanuele, C., James, C.J., Sonuga-Barke, E.J.S., 2007. Distinguishing low frequency oscillations within the 1/f spectral behaviour of electromagnetic brain signals. Behav. Brain Funct. 3.
Doesburg, S.M., Bedo, N., Ward, L.M., 2016. Top-down alpha oscillatory network interactions during visuospatial attention orienting. Neuroimage 132, 512–519.
Endl, W., Walla, P., Lindinger, G., Lalouschek, W., Barth, F., Deecke, L., Lang, W., 1998. Early cortical activation indicates preparation for retrieval of memory for faces: an event-related potential study. Neurosci. Lett. 240, 58–60.
Ergenoglu, T., Demiralp, T., Bayraktaroglu, Z., Ergen, M., Beydagi, H., Uresin, Y., 2004. Alpha rhythm of the EEG modulates visual detection performance in humans. Cogn. Brain Res. 20, 376–383.
Freeman, W.J., Holmes, M.D., Burke, B.C., Vanhatalo, S., 2003. Spatial spectra of scalp EEG and EMG from awake humans. Clin. Neurophysiol. 114, 1053–1068.
Gao, R., Peterson, E.J., Voytek, B., 2017. Inferring synaptic excitation/inhibition balance from field potentials. Neuroimage 158, 70–78.

Grandy, T.H., Werkle-Bergner, M., Chicherio, C., Lovden, M., Schmiedek, F., Lindenberger, U., 2013. Individual alpha peak frequency is related to latent factors of general cognitive abilities. Neuroimage 79, 10–18.
Haegens, S., Handel, B.F., Jensen, O., 2011. Top-down controlled alpha band Activity in somatosensory areas determines behavioral performance in a discrimination task. J. Neurosci. 31, 5197–5204.
Haegens, S., Osipova, D., Oostenveld, R., Jensen, O., 2010. Somatosensory working memory performance in humans depends on both engagement and disengagement of regions in a distributed network. Hum. Brain Mapp. 31, 26–35.
Haller, M., Donoghue, T., Peterson, E., Varma, P., Sebastian, P., Gao, R., Noto, T., Knight, R.T., Shestyuk, A., Voytek, B.J.b., 2018. Parameterizing Neural Power Spectra, 299859.
Hanslmayr, S., Aslan, A., Staudigl, T., Klimesch, W., Herrmann, C.S., Bäuml, K.-H., 2007. Prestimulus oscillations predict visual perception performance between and within subjects. Neuroimage 37, 1465–1473.
He, B.J., Zempel, J.M., Snyder, A.Z., Raichle, M.E., 2010a. The temporal structures and functional significance of scale-free brain activity. Neuron 66, 353–369.
He, B.Y.J., 2014. Scale-free brain activity: past, present, and future. Trends Cogn. Sci. 18, 480–487.
He, B.Y.J., Zempel, J.M., Snyder, A.Z., Raichle, M.E., 2010b. The temporal structures and functional significance of scale-free brain activity. Neuron 66, 353–369.
Heathcote, A., Popiel, S.J., Mewhort, D., 1991. Analysis of response time distributions: an example using the Stroop task. Psychol. Bull. 109, 340–347.
Herzmann, G., Kunina, O., Sommer, W., Wilhelm, O., 2010. Individual differences in face cognition: brain–behavior relationships. J. Cogn. Neurosci. 22, 571–589.
Hesse, J., Gross, T., 2014. Self-organized criticality as a fundamental property of neural systems. Front. Syst. Neurosci. 8.
Ikkai, A., Dandekar, S., Curtis, C.E., 2016. Lateralization in alpha-band oscillations predicts the locus and spatial distribution of attention. PLoS One 11.
Klimesch, W., 1999. EEG alpha and theta oscillations reflect cognitive and memory performance: a review and analysis. Brain Res. Rev. 29, 169–195.
Klimesch, W., Doppelmayr, M., Hanslmayr, S., 2006. Upper alpha ERD and absolute power: their meaning for memory performance. Event-Relat. Dyn. Brain Oscil. 159, 151–165.
Klimesch, W., Sauseng, P., Hanslmayr, S., 2007. EEG alpha oscillations: the inhibition-timing hypothesis. Brain Res. Rev. 53, 63–88.
Kornrumpf, B., Dimigen, O., Sommer, W., 2017. Lateralization of posterior alpha EEG reflects the distribution of spatial attention during saccadic reading. Psychophysiology 54, 809–823.
Lange, J., Halacz, J., van Dijk, H., Kahlbrock, N., Schnitzler, A., 2012. Fluctuations of prestimulus oscillatory power predict subjective perception of tactile simultaneity. Cerebr. Cortex 22, 2564–2574.
Larson, G.E., Alderton, D.L., 1990. Reaction time variability and intelligence: a 'worst performance' analysis of individual differences. Intelligence 14, 309–325.
Linden, H., Pettersen, K.H., Einevoll, G.T., 2010. Intrinsic dendritic filtering gives low-pass power spectra of local field potentials. J. Comput. Neurosci. 29, 423–444.
Linkenkaer-Hansen, K., Nikulin, V.V., Palva, S., Ilmoniemi, R.J., Palva, J.M., 2004. Prestimulus oscillations enhance psychophysical performance in humans. J. Neurosci. 24, 10186–10190.
Luce, R.D., 1986. Response Times: Their Role in Inferring Elementary Mental Organization. Oxford University Press, New York.
Lundqvist, D., Flykt, A., Öhman, A., 1998. The Karolinska Directed Emotional Faces (KDEF). CD ROM from Department Of Clinical Neuroscience, Psychology Section. Karolinska Institutet.
Mahjoory, K., Cesnaite, E., Hohlefeld, F.U., Villringer, A., Nikulin, V.V., 2019. Power and temporal dynamics of alpha oscillations at rest differentiate cognitive performance involving sustained and phasic cognitive control. Neuroimage 188, 135–144.
Markovic, D., Gros, C., 2014. Power laws and self-organized criticality in theory and nature. Phys. Rep. Rev. Phys. Lett. 536, 41–74.
Massidda, D., 2013. Retimes: Reaction Time Analysis. R Package Version 0.1-2. Available online: https://CRAN.R-project.org/package=retimes. (Accessed 21 March 2016).
McDonnell, M.D., Ward, L.M., 2011. The benefits of noise in neural systems: bridging theory and experiment. Nat. Rev. Neurosci. 12, 415–426.
Meisel, C., Storch, A., Hallmeyer-Elgner, S., Bullmore, E.T., Gross, T., 2012. Failure of adaptive self-organized criticality during epileptic seizure attacks. PLoS Comput. Biol. 8.
Miller, K.J., Sorensen, L.B., Ojemann, J.G., den Nijs, M., 2009. Power-law scaling in the brain surface electric potential. PLoS Comput. Biol. 5.
Muthukumaraswamy, S.D., Liley, D.T.J., 2018. 1/f electrophysiological spectra in resting and drug-induced states can be explained by the dynamics of multiple oscillatory relaxation processes. Neuroimage 179, 582–595.
Palva, J.M., Zhigalov, A., Hirvonen, J., Korhonen, O., Linkenkaer-Hansen, K., Palva, S., 2013. Neuronal long-range temporal correlations and avalanche dynamics are correlated with behavioral scaling laws. Proc. Natl. Acad. Sci. U.S.A. 110, 3585–3590.
Palva, S., Palva, J.M., 2007. New vistas for alpha-frequency band oscillations. Trends Neurosci. 30, 150–158.
Parameshwaran, D., Thiagarajan, T.C., 2017. Modernization, Wealth and the Emergence of Strong Alpha Oscillations in the Human EEG, 125898 bioRxiv.
Petro, N.M., Thigpen, N.N., Garcia, S., Boylan, M.R., Keil, A., 2019. Pre-target alpha power predicts the speed of cued target discrimination. Neuroimage 189, 878–885.
Pivik, R.T., Broughton, R.J., Coppola, R., Davidson, R.J., Fox, N., Nuwer, M.R., 1993. Guidelines for the recording and quantitative analysis of electroencephalographic activity in research contexts. Psychophysiology 30, 547–558.
Podvalny, E., Noy, N., Harel, M., Bickel, S., Chechik, G., Schroeder, C.E., Mehta, A.D., Tsodyks, M., Malach, R., 2015. A unifying principle underlying the extracellular field potential spectral responses in the human cortex. J. Neurophysiol. 114, 505–519.
Pritchard, W.S., 1992. The brain in fractal time - 1/F-like power spectrum scaling of the human electroencephalogram. Int. J. Neurosci. 66, 119–129.
Rosseel, Y., 2012. Lavaan: an R package for structural equation modeling. J. Stat. Softw. 48, 1–36.
Schmiedek, F., Oberauer, K., Wilhelm, O., Suess, H.-M., Wittmann, W.W., 2007. Individual differences in components of reaction time distributions and their relations to working memory and intelligence. J. Exp. Psychol. Gen. 136, 414–429.
Schmitz, F., Wilhelm, O., 2016. Modeling mental speed: decomposing response time distributions in elementary cognitive tasks and relations with working memory capacity and fluid intelligence. J. Intell. 4, 1–23.
Steiger, J.H., 1980. Statistically Based Tests for the Number of Common Factors. The Annual Meeting of the Psychometric Society. Iowa City, IA, 1980.
Tagliazucchi, E., von Wegner, F., Morzelewski, A., Brodbeck, V., Jahnke, K., Laufs, H., 2013. Breakdown of long-range temporal dependence in default mode and attention networks during deep sleep. Proc. Natl. Acad. Sci. U.S.A. 110, 15419–15424.
Tallon-Baudry, C., Bertrand, O., 1999. Oscillatory gamma activity in humans and its role in object representation. Trends Cogn. Sci. 3, 151–162.
Thut, G., Nietzel, A., Brandt, S.A., Pascual-Leone, A., 2006. alpha-Band electroencephalographic activity over occipital cortex indexes visuospatial attention bias and predicts visual target detection. J. Neurosci. 26, 9494–9502.
Unsworth, N., Redick, T.S., Lakey, C.E., Young, D.L., 2010. Lapses in sustained attention and their relation to executive control and fluid abilities: an individual differences investigation. Intelligence 38, 111–122.
Valizadeh, S.A., Riener, R., Elmer, S., Jäncke, L., 2019. Decrypting the electrophysiological individuality of the human brain: identification of individuals based on resting-state EEG activity. Neuroimage 197, 470–481.
Van de Ville, D., Britz, J., Michel, C.M., 2010. EEG microstate sequences in healthy humans at rest reveal scale-free dynamics. Proc. Natl. Acad. Sci. U.S.A. 107, 18179–18184.
Van Dijk, H., Schoffelen, J.M., Oostenveld, R., Jensen, O., 2008. Prestimulus oscillatory activity in the alpha band predicts visual discrimination ability. J. Neurosci. 28, 1816–1823.
Van Zandt, T., 2000. How to fit a response time distribution. Psychon. Bull. Rev. 7, 424–465.
Voytek, B., Knight, R.T., 2015. Dynamic network communication as a unifying neural basis for cognition, development, aging, and disease. Biol. Psychiatry 77, 1089–1097.
Voytek, B., Kramer, M.A., Case, J., Lepage, K.Q., Tempesta, Z.R., Knight, R.T., Gazzaley, A., 2015. Age-related changes in 1/f neural electrophysiological noise. J. Neurosci. 35, 13257–13265.
Wang, X.J., 2010. Neurophysiological and computational principles of cortical rhythms in cognition. Physiol. Rev. 90, 1195–1268.
Waschke, L., Wostmann, M., Obleser, J., 2017. States and traits of neural irregularity in the age-varying human brain. Sci. Rep. 7.
Weisz, N., Wuhle, A., Monittola, G., Demarchi, G., Frey, J., Popov, T., Braun, C., 2014. Prestimulus oscillatory power and connectivity patterns predispose conscious somatosensory perception. Proc. Natl. Acad. Sci. U. S. A. 111, E417–E425.
Wen, H.G., Liu, Z.M., 2016a. Broadband electrophysiological dynamics contribute to global resting-state fMRI signal. J. Neurosci. 36, 6030–6040.
Wen, H.G., Liu, Z.M., 2016b. Separating fractal and oscillatory components in the power spectrum of neurophysiological signal. Brain Topogr. 29, 13–26.
Worden, M.S., Foxe, J.J., Wang, N., Simpson, G.V., 2000. Anticipatory biasing of visuospatial attention indexed by retinotopically specific alpha-band electroencephalography increases over occipital cortex. J. Neurosci. 20, RC63.
Yamamoto, Y., Hughson, R.L., 1993. Extracting fractal components from time-series. Physica D 68, 250–264.
Zhang, Y., Ding, M.Z., 2010. Detection of a weak somatosensory stimulus: role of the prestimulus Mu rhythm and its top-down modulation. J. Cogn. Neurosci. 22, 307–322.